Hindawi
Journal of Food Quality
Volume 2022, Article ID 6947775, 10 pages
https://doi.org/10.1155/2022/6947775

Research Article

Rapid Trace Detection of Pesticide Residues on Tomato by Surface-Enhanced Raman Spectroscopy and Flexible Tapes

Mingzhu Tao,[1] **Hui Fang**,[1,2] **Xuping Feng**,[1] **Yong He**,[1] **Xiaoxi Liu**,[1] **Yongqiang Shi**,[1] **Yuzhen Wei**,[3] **and Zhiqi Hong**[4]

[1]*Huanan Industrial Technology Research Institute of Zhejiang University, Guangzhou 510700, China*
[2]*Digital Village Laboratory, Huzhou Institute of Zhejiang University, Huzhou 313099, China*
[3]*School of Information Engineering, Huzhou University, Huzhou 313000, China*
[4]*The Rural Development Academy & Agricultural Experiment Station, Zhejiang University, Hangzhou 310058, China*

Correspondence should be addressed to Zhiqi Hong; hzq@zju.edu.cn

Received 23 February 2022; Accepted 29 April 2022; Published 13 May 2022

Academic Editor: Yuxia Fan

The non-judicious use of pesticides in agro-food poses a severe threat to food safety and human health. As an emerging chromatographic fingerprint provider, surface-enhanced Raman spectroscopy analysis (SERS) sheds bright light on sensitive and nondestructive detection of pesticide residues. This research proposed a novel strategy to detect three-pesticide residues (thiabendazole, carbendazim, and chlorpyrifos) on tomato peel based on the flexible and sticky SERS substrate. After selecting the best commercial adhesive tape (3M9080), the SERS substrate was constructed by optimizing the parameters in the preparation process of AuNPs. Therefore, a new simple "tape-wrapped SERS" way for pesticide residue analysis was established with a simple procedure of "absorption, separation, and drop addition." Based on chemometrics method, the limit of semiquantitative detection was 20, 36, and 80 ng/cm^2 for thiabendazole, carbendazim, and chlorpyrifos, respectively, on tomato surface, which indicated that the proposed method could meet the requirement of actual application with a large prospect in agro-food safety detection.

1. Introduction

Reasonable use of pesticides is beneficial to yield increase, but overuse will lead to a boost in excessive pesticide residues and food safety problems. Tomato is a widely grown crop with nutritional value and medicinal value; for example, lycopene was proven to reduce the risk of numerous cancers [1]. A great number of pesticides are used in tomato production to guarantee considerable yield and quality. For example, thiabendazole, carbendazim, and chlorpyrifos are broad-spectrum pesticides and are used for control of fungal diseases [2, 3]. However, pesticide residues on tomatoes are toxic to humans' health, so they need to be strictly checked from the farm to the market. Different countries have also introduced maximum residue limit (MRL) standards for pesticides to ensure food safety. The value of MRL for the same pesticide on tomato surface varies with the standard. Besides, not all pesticides' MRLs on tomato surface are clearly defined. For example, China, the European Union, and Japan set MRL of carbendazim on tomato surface to 3, 0.3, and 3 mg/kg, respectively, while the United States does not specify it. Currently, in most standards, high performance liquid chromatography (HPLC) is used to measure pesticide residues with the advantage of high sensitivity and accuracy [4]. However, this mature technology always requires sophisticated sample pretreatments, complicated operating procedures, expensive testing instruments, and labor costs, making it unsuitable for online and high throughput screening.

As a versatile sensitive vibrational spectroscopy technique, surface-enhanced Raman scattering (SERS) is capable of detecting low concentration analytes after the amplification of electromagnetic fields generated by the excitation of localized surface plasmons [5]. SERS achieves a greater enhancement (10^6–10^8) and makes up of the feeble signals of normal typical Raman scattering by adsorbing the analyte

molecule onto a roughened metal surface [6]. In the past decades, SERS technique was widely adopted in the trace detection of pesticide content [2, 7–10]. This research on the fabrication of highly stable and sensitive SERS substrates has been the driving force for the continuous progress of SERS technology for pesticide residue detection. Owing to the lack of elasticity and conformal sampling on irregular surfaces, some conventional SERS substrates become the main restriction in the practical agro-food application. Hence, flexible materials including polymer film, adhesive tape, cotton swabs, and filter paper [11–14] have attracted considerable attention in fabricating flexible SERS substrates, which contribute to a firm fix on the analyte in a facile way. For example, Chen et al. [15] proposed a viable and simple "paste and peel-off" procedure to detect pesticide residues in complex agro-food surfaces with 3M transparent adhesive tape as the SERS substrate. To overcome the uneven distribution of gold nanoparticles on tape, a novel "tape-wrapped SERS" method was demonstrated by Jiang et al. [16] through the "paste peel, and paste again" procedure; trace detection of pesticide residues was rapidly achieved with a portable Raman spectrometer.

Although the promising results of applying flexible SERS substrate to detect pesticide residues on the complex agro-food surface have been reported one by one, there are still many challenges on the road from laboratory test results to everyday practical applications. One of the crucial challenges is that the preparation of flexible SERS substrates usually requires complicated procedures, and the morphology of nanoparticles is not easy to control [17, 18]. In terms of flexible materials, most of them have no viscosity, which leads to unsatisfactory results like low sampling rate and suboptimal detection [19]. Apart from these, the quantitative analysis accuracy should be further improved [20]. To our knowledge, pesticide residue detection on the fruits and vegetables surface with flexible SERS substrate generally stays in the qualitative or semiquantitative analysis. Among these research works, just a single characteristic peak is chosen, which is easy susceptibility to nonlinear factors such as instruments and environmental noise [21].

Herein, we demonstrated a tape-wrapped SERS method by utilizing the properties of the substrate to be specific, combining the stickiness and flexibility of the adhesive tape and the SERS activity of AuNPs. The specific goals were as follows: (1) to select the commercial adhesive tape with the best performance as SERS tape by investigating SERS activity and sampling rate; (2) to optimize the concentration of AuNPs and coagulants for SERS substrate; (3) to build an optimal regression model with high accuracy for each pesticide detected; (4) to realize the rapid pesticide residue detection on tomato surfaces.

2. Materials and Methods

2.1. Chemicals and Materials. Thiabendazole standard (98.4%) was provided by National Pesticide Quality Supervision and Testing Center, carbendazim standard (98.1%) and chlorpyrifos standard (99.4%) were obtained from China Standard Material Network, and the other reagents (e.g., methanol, trisodium citrate, HAuCl4, NaCl, NaBr) were purchased from Sinopharm Chemical Reagent Co., Ltd. (Shanghai, China). All reagents were used without further purification. Ultrapure water (Millipore, ≥18 MΩ cm^{-1}) was used for all experiments.

As shown in Figure S1, four commercial tapes (scotch tape, paper tape, 3M Post-it, 3M9080 super tape) were purchased from the local supermarket, Hangzhou, China. Tomatoes were brought from Shandong, China, with uniform size (approximately sphere) and no obvious mechanical damage.

2.2. Gold Nanoparticles (AuNPs) Preparation and Characterization. The AuNPs were fabricated according to the method adopted by previous literature with slight modification [22]. Specifically, $HAuCl_4$ (100 mL, 0.01%, 0.3 mM) was heated to boiling at 120 °C on a constant temperature magnetic stirrer. Then, 0.5 mL trisodium citrate solution (1%) was added quickly. After 25 minutes of stirring, the solution was cooled naturally at room temperature and stored at 4°C for subsequent experiments. To obtain different concentrations of AuNPs, the specific procedure was as follows. 30 mL of as-prepared AuNPs was centrifuged at 4500 rpm for 10 minutes to remove the supernatant. By repeating the above steps, the remaining colloid volumes in the lower layer were 24 mL, 18 mL, 12 mL, and 6 mL, respectively. Vortex oscillator was used to make the colloid mixing evenly, and five concentrated AuNPs (1.25, 1.67, 2.5, 5 times) were obtained. The surface morphology of the AuNPs on adhesive tape was observed by Scanning electron microscopy (SEM, Gemini SEM 300).

2.3. Sample Preparation. In our experiments, tomatoes were washed with ultrapure water carefully after soaking in ultrapure water for 30 minutes and dried naturally in air. As shown in Figure 1, 40 μL of pesticide (thiabendazole, carbendazim, and chlorpyrifos) standard solution (5 mg/L) was spread on the tomato peel (~1 cm^2). After the pesticide solution was completely dried at room temperature, the commercial adhesive tape was pasted on the corresponding area with a regular pressure using a rubber scraper for 15 s to ensure the analytes were fully translated, and peeled off discreetly. Then, the tapes containing analytes were divided into two groups to measure pesticide content, one group were carried out by high performance liquid chromatography (HPLC, Agilent 1200, Agilent, USA), and the other group were dropped with AuNPs and coagulants in turn, for further SERS measurement. It is worth mentioning that different concentrating times (1, 1.25, 1.67, 2.5, 5 times) and amounts (40, 80, 120, 160 μL) of AuNPs, different candidates (1% NaBr, 1% NaCl), and different volumes (1, 5, 10, 15, 20 μL) of coagulants were prepared to optimize SERS results.

2.4. Raman Spectra Acquisition. Raman spectra were recorded before the solvent (AuNPs and coagulants) completely evaporated, and were carried out by a RmTracer-200-HS portable Raman spectrometer combined with a 785 nm

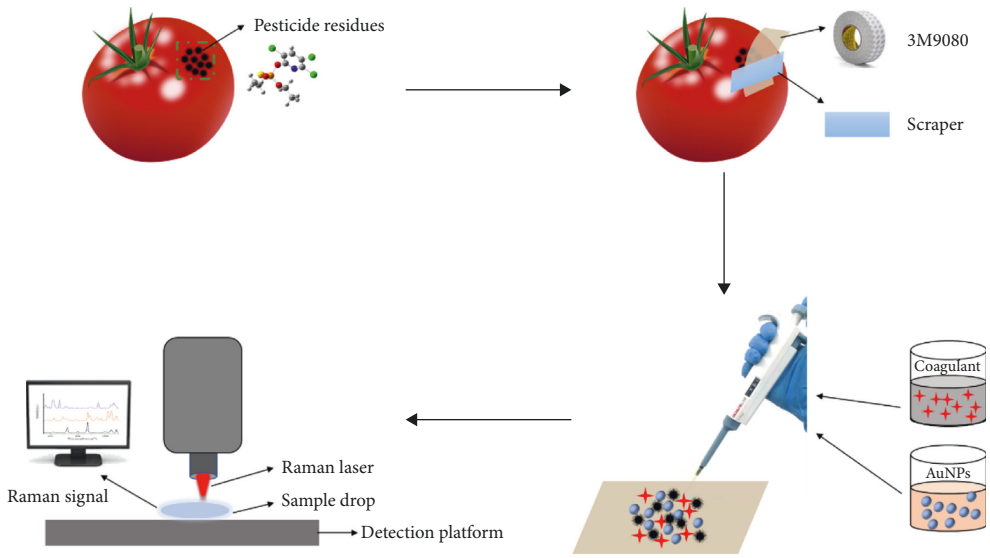

Figure 1: Sampling and detection process of pesticide residues on tomato surface based on flexible surface-enhanced Raman scattering (SERS) substrate.

excitation wavelength diode-stabilized stimulator (Opto Trace Technologies, Inc., Silicon Valley, CA, USA). Notably, the instrument should be calibrated using a 785 nm excitation wavelength before Raman spectra acquisition. The parameters were set as follows: power of 200 mW; scanning range from 200 to 3300 cm^{-1}; an optical resolution of 2 cm^{-1}; and integration time, number of exposures, and smooth coefficient adjusted to 10 s, 5 times, and 1, respectively.

2.5. Density Functional Theory (DFT). Density functional theory (DFT), as a quantum mechanical calculation method based on the electronic structure of multielectron systems, is the most common approach to study the electronic structure of multielectron systems. Currently, it has been widely used to study the properties of molecules for identifying characteristic peaks [23]. In this research, the optimization of the molecular structure of pesticides was carried out on GaussView 6.0 (Gaussian, Inc., Wallingford, CT, USA), the calculation of theoretical Raman spectra of pesticides molecular was implemented on Gaussian 09 (Gaussian, Inc., Wallingford, CT, USA), and correction of Raman spectra baseline was carried out on OMNIC v8.2 (infrared spectrum processing software, Thermo Fisher Scientific, USA).

To identify the characteristic peaks accurately, the results simulated by DFT were compared with the SERS of each pesticide standard solution.

2.6. Modeling Methods, Evaluation Indices, and Software. In this step, the least squares support vector machine (LSSVM) was selected to implement pesticide detection predictive mode based on the Raman spectra. LSSVM maps the input variables of low dimension space to those of high dimension space through a nonlinear method, transforms the unequal constraints in SVM into equal constraints, and realizes the optimization based on Lagrange method, which can better deal with the nonlinear factors [24]. To improve the compute speed and prediction accuracy, the radial basis function (RBF) was selected to optimize the regularization parameter (γ) and the kernel parameter (σ^2) in the nonlinear discrimination. The performance of the LSSVM model was evaluated by the coefficient of determination (R^2), root mean square error (RMSE), and residual predictive deviation (RPD), and the subscripts c and p in these indices represented the calibration set and the prediction set, respectively.

In this research, B3LYP/6-31G (d, p) was used to simulate and calculate three pesticide molecules in Gaussian 09 software. LSSVM was conducted on MATLAB R2018a (MathWorks, Natick, MA, USA), and spectrum preprocessing was performed on Unscrambler® 10.1 (CAMO AS, Oslo, Norway), a one-way analysis of variance (ANOVA), was conducted by using SPSS V.22 statistical software (SPSS Inc., Chicago, IL, USA), and all figures were realized by OriginPro 2018 (OriginLab Corporation, Northampton, MA, USA).

3. Results and Discussion

3.1. Three Pesticides' SERS and Its Assignment of Raman Peaks. The first step of pesticide content detection is to attribute Raman peaks for each one. In this part, three pesticide molecular structures were simulated in Gaussian 09 software (Figure 2(a)). DFT-calculated Raman peak, solid pesticide Raman spectra, and corresponding solution (dissolved in acetonitrile) SERS were contrasted to verify the matching degree between the theory and experiment to assign Raman peaks accurately. By analyzing the difference between Raman spectra of the standard solids and solution, the solvent disturbance can be determined to some extent. Furthermore, the interference from external environment and pesticide purified can be identified from the results of DFT-calculated and the other two. As shown in Figure 2(b), DFT-calculated Raman spectra of thiabendazole had strong Raman activity at 783, 1009, and 1264 cm^{-1}. Compared with

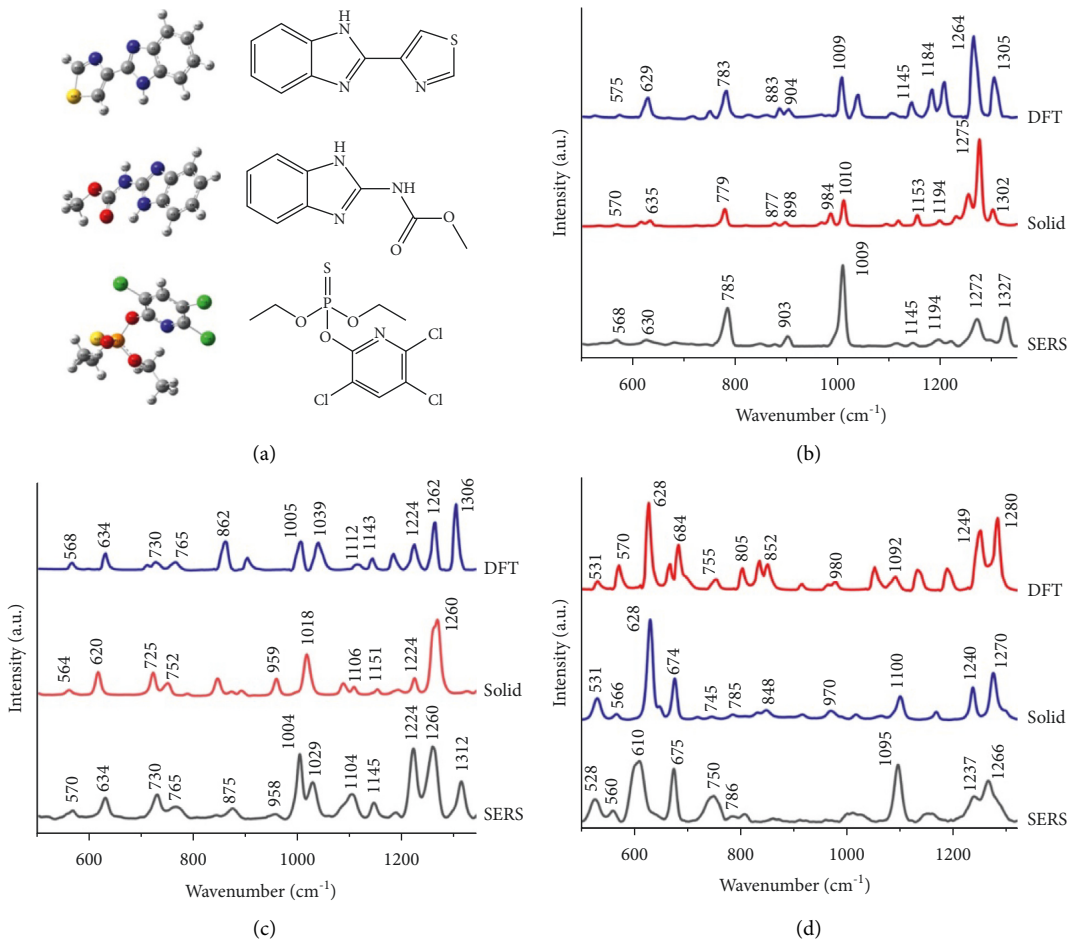

Figure 2: (a) the simulated molecular structure. Raman spectra of (b) thiabendazole, (c) carbendazim, and (d) chlorpyrifos. The blue line represents the density functional theory (DFT)-calculated Raman spectra of the pesticide. The red line represents Raman spectra of the pesticide solid. The black line represented SERS spectra of the pesticide solution.

the Raman spectra at 785, 1009 cm^{-1} of solid thiabendazole, SERS of its solution had significant stronger intensity, which was assigned to C-H deformable vibration and outer surface bending [25]. Carbendazim exhibited various molecular vibration modes and complex Raman peaks (Figure 2(c)). At the range of 500 ~ 1000 cm^{-1}, although the intensity of three spectra were weak, there were good correspondence between the peak positions. At the range of 1000 ~ 1400 cm^{-1}, some spectra peaks exhibited the phenomenon of merger and shift. Compared to solid carbendazim Raman, SERS of its solution was enhanced greatly at 1004, 1029, and 1312 cm^{-1}. The peak at 1004 cm^{-1} was assigned to C-O stretching vibration. The peak at 1029 cm^{-1} was assigned to C-C stretching and H-C-C bending vibration. The peak at 1312 cm^{-1} was assigned to C-N stretching vibration [26]. From Figure 2(d), the three Raman spectra had a high matching degree. Stronger enhancement was obtained mainly at 610 (*P*=*S* and C-Cl stretching vibrations), 675 (benzene ring breathing vibration), 750 (P-O-C stretching vibration), and 1095 cm^{-1} (benzene ring and *C*=*N* stretching vibration) compared to solid Raman spectra [27]. As a result, both of the solid pesticide Raman spectra and their solution SERS were basically consistent with DFT-calculated Raman peaks with a reasonable range of Raman shifts (within 15 cm^{-1}), so these peaks could be used as the corresponding feature peaks. The detailed attribution of Raman spectra of the three pesticides is shown in Tables S1–S3.

3.2. Selection of Commercial Adhesive Tape. Cheap adhesive tape has received great interest and been applied in preparing SERS substrates. Although its stickiness enables nanoparticles to be fully fixed on it and target analytes to be loaded easily, the inherent properties like background fluorescence would play a considerable role in SERS signals. Four commercial adhesive tapes (scotch tape, paper tape, 3M Post-it, 3M9080 super tape) were investigated under uniform experimental conditions, respectively. The results were listed in Figure 3. Compared to the SERS spectra of paper tape and 3M Post-it, 3M9080 and scotch tape showed a satisfactory consequence both in number and sites of characteristic peaks (Figures 3(a)–3(c)). These two tapes also exhibited low background inference, potentially owing to the intrinsic property of the coated film [15]. Paper tape failed in the characterization of carbendazim and chlorpyrifos with weak SERS intensity and strong noise, and 3M Post-it

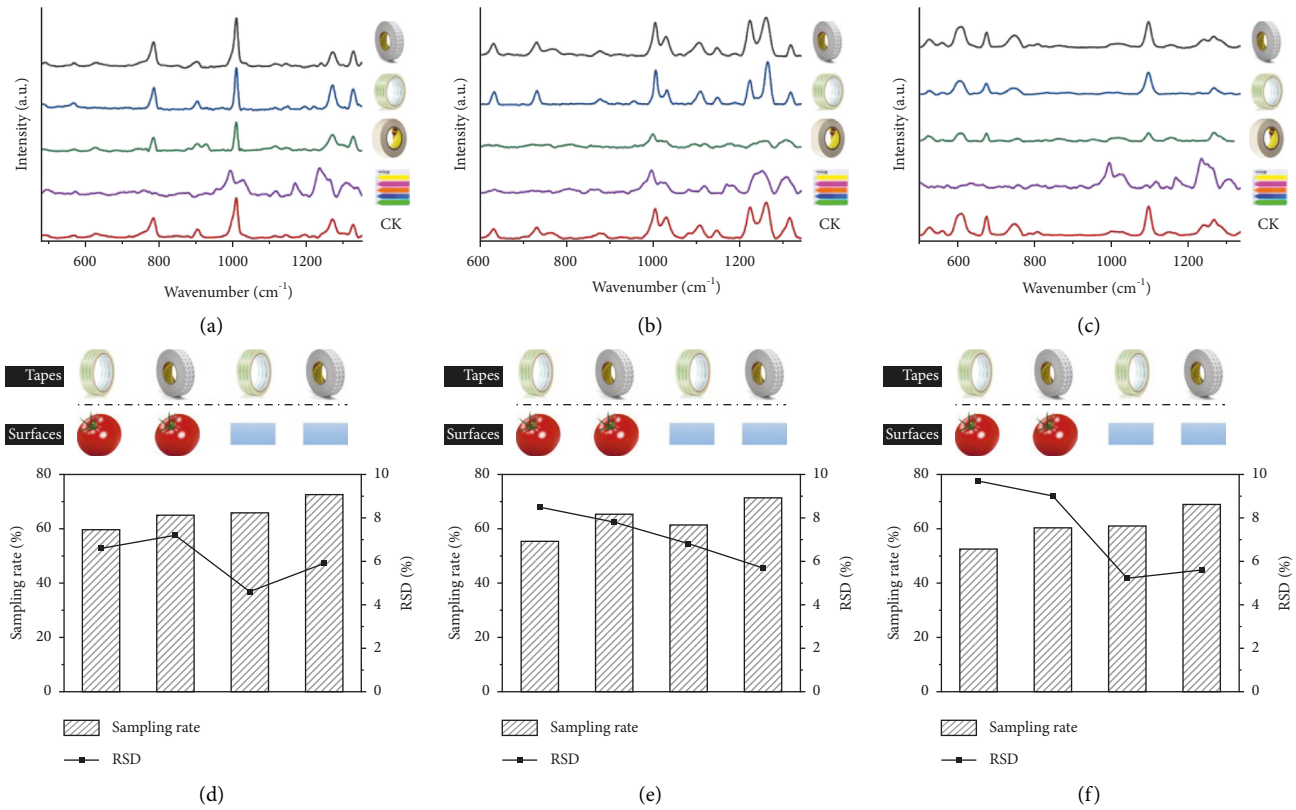

Figure 3: Raman spectra of (a) thiabendazole, (b) carbendazim, and (c) chlorpyrifos on different commercial tapes. Sampling performance of (d) thiabendazole, (e) carbendazim, and (f) chlorpyrifos collected from different surfaces on different commercial tapes. CK represents surface-enhanced Raman spectra of the corresponding pesticide solution.

showed little potential for pesticide residue detection, possibly due to weak viscosity and intense fluorescence. Besides, the pesticide affinity of AuNPs also affected the enhancement of flexible SERS substrate.

To evaluate SERS performance of 3M9080 and scotch tape, the sampling rate [28] was defined by the mass ratio of the value from HPLC and the actual addition amount, which was measured 12 times and averaged between them. The results are exhibited in Figures 3(d)–3(f). Compared with glass surface, the experiment with tomato peels got lower sampling rate and higher RSD, which might be attributed to tomato uneven surface and a small amount of pesticide infiltration through tomato peel. Table S4 proved the type of adhesive tape had a significant effect on the sampling rate ($P < 0.01$). 3M9080 showed higher sampling rate and lower RSD value compared to scotch tape and was selected as a substrate of SERS tape for further analysis.

3.3. Optimization of Flexible SERS Substrate. Apart from the inherent attributes of adhesive tape, the concentration, dosage, and variety of ingredients of SERS substrate also affect the intensity of SERS signal. In this research, the concentrating time and dosage of AuNPs, and type and dosage of coagulants were tested. For each pesticide, according to the intensity and shift of Raman spectra, only several characteristic peaks were selected (thiabendazole: 785 and 1009 cm^{-1}; carbendazim: 1224 and 1260 cm^{-1}; chlorpyrifos: 610 and 675 cm^{-1}). Figure 4 illustrated the SERS spectra intensity affected by the different density and variety of ingredients for fabricating a suitable SERS substrate for each pesticide. For the three pesticides, in the beginning, higher AuNPs concentration and stronger SERS signal were obtained (Figures 4(a)–4(c)), which was consistent with other studies [29]. Moreover, with the concentration continuing to increase, the signal began to weaken. This result might be explained by the fact that low concentration of AuNPs made it hard to contact with the target molecules entirely, while high concentration might lead to the agglomeration of metal particles caused by smaller distance and nonideal enhancement owing to the weak ability to generate SERS "hot spots" [30].

It is widely accepted that activating ions such as Cl^- and Br^- could enhance SERS signal due to NPs aggregation induced hot spots [31, 32], it is also well known that aggregation is relatively random, which could produce large variation in repeatability. Thus, the above concerns will be discussed in detail. In this research, NaBr and NaCl were studied (Figures 4(d)–4(f)). In terms of SERS signal intensity, NaCl was the best one for the three pesticides because its addition made the colloids reach a more suitable condensation state to generate more "hot spots." To further investigate the aggregation effect introduced by NaCl, the characterization was carried out by an ultraviolet spectrophotometer (Figure S2). After the addition of NaCl, the

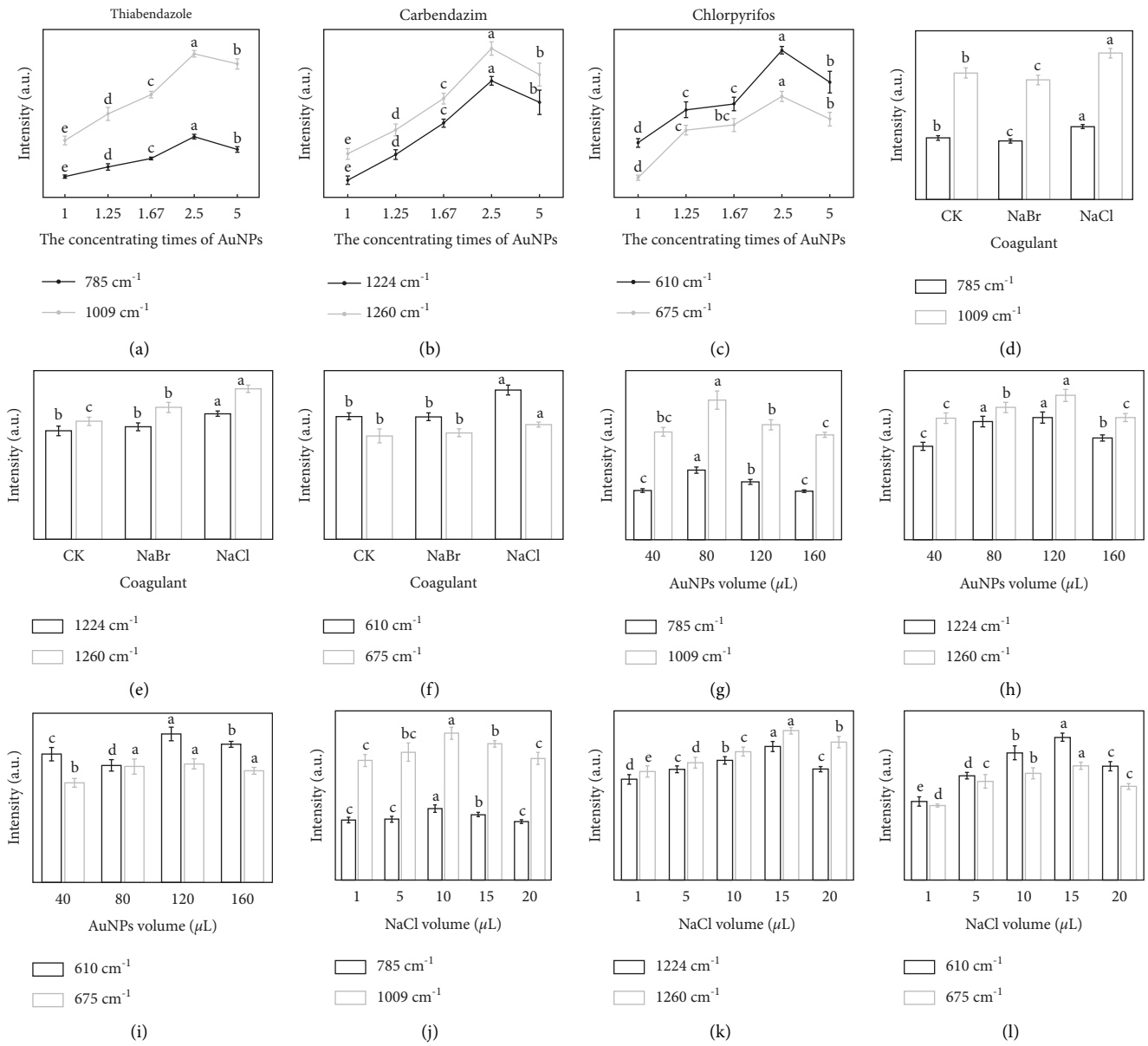

Pesticide	The concentrating times of AuNPs	Coagulant	The dosage of AuNPs	The dosage of coagulant
Thiabendazole	2.5	NaCl	80 μL	10 μL
Carbendazim	2.5	NaCl	120 μL	15 μL
Chlorpyrifos	2.5	NaCl	120 μL	15 μL

(m)

Figure 4: SERS signal of characteristic peaks with (a–c) different AuNPs concentrations, (d–f) different coagulants, (g–i) different AuNPs dosages, and (j–l) different NaCl dosages. (m) Summary of optimal parameters for each pesticide. CK represents the group without coagulants. (a), (d), (g), (j) The results of thiabendazole; (b), (e), (f), (k) the results of carbendazim; (c), (f), (i), (l) the results of chlorpyrifos. Different color depths represent different characteristic peaks. Bars and points indicate the means ± standard deviation of eight replicates. Within the same characteristic peak, any two bars or points with different letters are statistically significant according to ANOVA (Tukey post hoc test, $P < 0.05$).

maximum absorption peak of AuNPs was shifted from 530 nm to 540 nm, which related to the size of the nanoparticles [21]. The energy gap between the occupied and unoccupied molecular orbitals diminished with the increase of particle diameter, which resulted in the light absorption band shift to long wave (red shift) [33]. Therefore, it could be inferred that with the addition of NaCl, the size of AuNPs increased by polymerization and precipitation, resulting in a red shift. Besides, as shown in Figure S3, the distribution of AuNPs without coagulant was relatively scattered, while it

showed obvious aggregation after dropping NaCl, which was consistent with the ultraviolet spectrum change. Then, the flexible SERS substrate SEM was conducted with NaCl, and AuNPs were close to each other and were distributed tightly and evenly on the tape (3M9080); namely, there were many uniformly distributed "hot spots." Therefore, NaCl was selected as a coagulant for subsequent research.

The amount of AuNPs also needed to be optimized since the amount of AuNPs would directly affect the number of "hot spots" according to the electromagnetic enhancement mechanism of SERS [34]. Like the concentration of AuNPs, the excellent SERS signal could not be realized with too much or too little dosage of AuNPs (Figures 4(g)–4(i)). As the amount increased, SERS signal improved first and then declined in general [35]. Specifically speaking, pesticide was absorbed onto AuNPs by multilayer superposition at a low level of AuNPs due to insufficient valid "hot spots." With the increase of the number of AuNPs, pesticide molecules had more access to "hot spots." When the number of AuNPs continued to increase, the particles would be excessively wrapped, which led to a relative decrease in the valid "hot spots." According to the results (Figures 4(g)–4(i)), for the detection of thiabendazole, carbendazim, and chlorpyrifos on tomato surface, the optimal amount of AuNPs was 80 μL, 120 μL, and 120 μL, respectively.

The dosage of NaCl influencing the aggregation degree of AuNPs [36, 37] was also studied at five dosages (1 μL, 5 μL, 10 μL, 15 μL, 20 μL). From Figures 4(j)–4(l), it was also a double-edged sword. In a certain range, as AuNPs were negatively charged, sodium ions in NaCl solution could neutralize their negative charge, which reduced the repulsion between nanoparticles and improved AuNPs aggregation, thus enhancing SERS signal. However, excessive NaCl would lead to excessive agglomeration of AuNPs. For thiabendazole, carbendazim, and chlorpyrifos, the optimum NaCl value was 10 μL, 15 μL, and 15 μL, respectively; namely, the dosage ratio of AuNPs to NaCl was 8 : 1. Finally, the optimal parameters can be concluded in Figure 4(m).

3.4. Sensitivity and Uniformity of SERS Tape. Sensitivity and uniformity of SERS substrate are the primary concerns about the evaluation of SERS performance. To study the sensitivity of the optimized flexible SERS substrate, different concentrations of standard pesticide solutions were deposited onto the sticky side of the adhesive tape (3M9080). After the solution was dried naturally, AuNPs and NaCl were successively added to attain Raman spectra. At the same time, the spectra of twenty detection sites were randomly collected on the flexible SERS substrate surface to investigate the uniformity.

As shown in Figure S4, the intensity of Raman characteristic peak gradually decreased with the reduction of the concentration. The SERS spectral feature peaks of thiabendazole at 785 and 1009 cm^{-1} were still observed even when the concentration reduced to 8 ng/cm^2 (Figure S4(a)). In the same way, the limits of detection concentration of carbendazim (Figure S4(b)) and chlorpyrifos (Figure S4(c)) were 20 and 40 ng/cm^2, respectively, which satisfied the linear relationship (coefficient of determination $(R^2) \geq 0.970$), indicating the good sensitivity of optimized SERS substrate. The RSD values of the three pesticides at the studied feature peaks were below 9% (Figure S5). Both the limit of detection concentration and RSD were lower than previous work [38], demonstrating the feasibility of the proposed strategy for pesticide residue detection on tomato surface. Stability was another remarkable feature of SERS tape. As one of the most important elements, the prepared AuNPs still worked well after 45 days, and they showed clear characteristic peaks (610 cm^{-1} and 675 cm^{-1}), which indicated that SERS tape could keep relative stability after long-term storage (Figure S6).

3.5. Application for Semiquantitative Pesticide Residue Detection from Tomato Surfaces. According to MRL standards in China, detection limits for thiabendazole, carbendazim, and chlorpyrifos are 5, 3, and 0.02 mg/kg (http://2763.foodvip.net/category/limit/136.html), respectively. The process of converting it to the maximum residues per unit area is as follows [16]. Each tomato is assumed to weigh 200 g and has a surface area of 180 cm^2; then, the maximum residues of thiabendazole per unit area = 5 mg/kg × 200 $g \times 10^3/180\ cm^2 = 5555\ ng/cm^2$, and the maximum residues of carbendazim and chlorpyrifos per unit area are 3333 ng/cm^2 and 22 ng/cm^2, respectively. Then, 10 mg of thiabendazole, carbendazim, and chlorpyrifos was dissolved in acetonitrile to prepare 100 mg/L standard solution. Then, it was diluted to 0–20 mg/L and kept away from light. 40 μL of the diluted standard solution was dropped onto 1 cm^2 of the cleaned tomato peel, and it was allowed to dry naturally. We selected 93 samples for each pesticide (concentration range: 0-800 ng/cm^2), and 279 samples of three pesticides altogether were divided into calibration set and prediction set in a ratio of 3 : 1.

On one flexible SERS tape, the Raman spectra from three different sites were selected randomly and averaged after baseline correction. With the different amount of pesticides added on the tomato surface, the characteristic peak intensity increased in varying degrees (Figure 5). Although the characteristic peak strength was very weak when the concentration of thiabendazole dropped to 20 ng/cm^2, the signal at 1009 cm^{-1} was still clearly visible, indicating that semiquantitative detection limit of thiabendazole residue on tomato surface could reach 20 ng/cm^2 by using flexible SERS substrate. In the same way, semiquantitative detection limits of carbendazim and chlorpyrifos on tomato surface with flexible SERS substrate were 36 and 80 ng/cm^2, respectively. Therefore, semiquantitative detection limits of thiabendazole and carbendazim on tomato surface were substantially lower than the MRLs required by the national standards. Although semiquantitative detection limit of chlorpyrifos did not meet MRL, it could be used for preliminary screening of tomatoes, which was equally important in quality testing. To sum up, the flexible SERS substrate is expected to bring the emerging SERS technology closer to everyday on-spot detection.

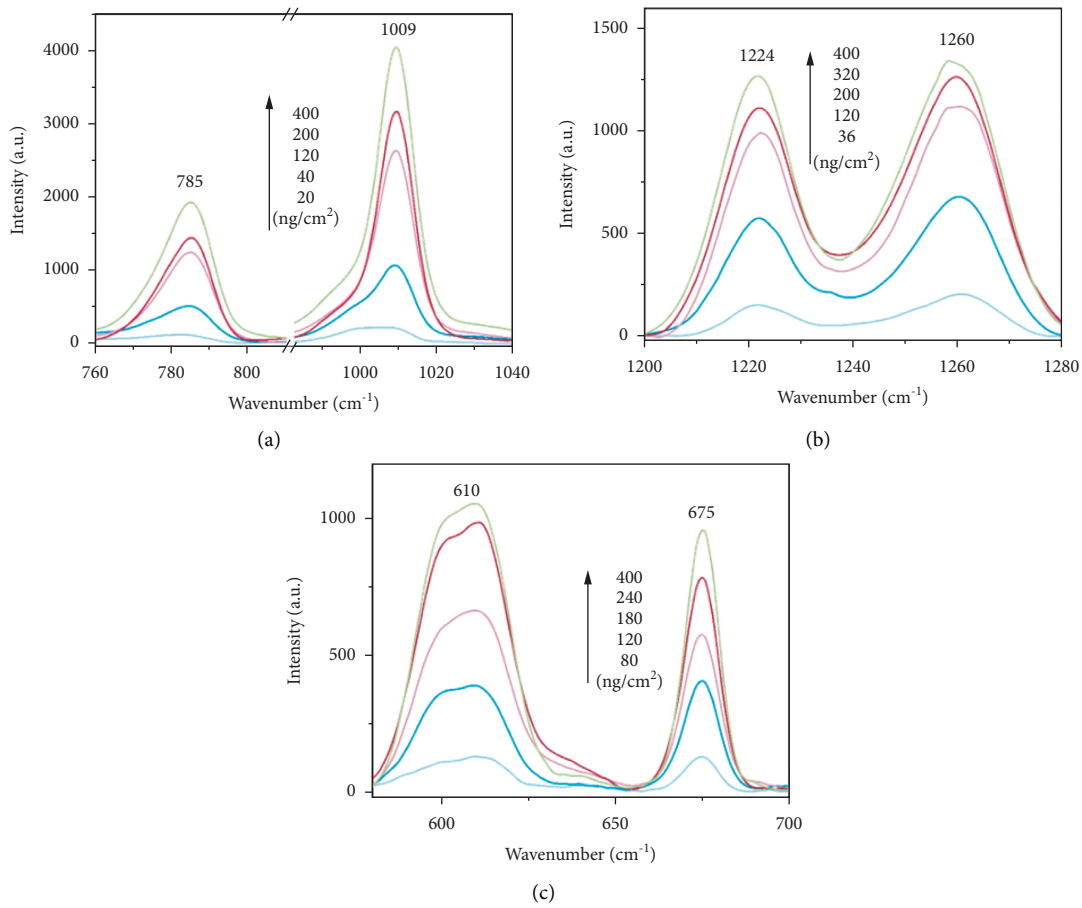

Figure 5: The selected SERS feature spectra of (a) thiabendazole, (b) carbendazim, and (c) chlorpyrifos on tomato under the five concentrations selected.

Table 1: Modeling results based on characteristic peak.

Pesticide	Characteristic peak band (cm^{-1})	Calibration set		Prediction set		
		R_C^2	$RMSE_C$ ($ng{\cdot}cm^{-2}$)	R_P^2	$RMSE_P$ ($ng{\cdot}cm^{-2}$)	RPD
Thiabendazole	760–800 LSSVM	0.972	31.944	0.960	36.103	5.004
	980–1020 LSSVM	0.995	13.253	0.887	56.138	3.111
Carbendazim	1200–1235 LSSVM	0.937	50.267	0.748	133.166	1.837
	1235–1280 LSSVM	0.993	17.498	0.933	68.922	3.504
Chlorpyrifos	580–630 LSSVM	0.985	25.668	0.864	92.847	2.507
	660–690 LSSVM	0.984	30.761	0.796	108.231	1.823

Furthermore, a slight peak shift occurred on SERS feature peaks at the low concentration (Figure 5), indicating it was not accurate to establish the model by using a single characteristic peak. In this section, LSSVM model was established with multiple bands near the characteristic peaks according to the attribution of Raman peak and signal intensity (Table 1). For thiabendazole, spectra of 760-800 cm^{-1} (near 785 cm^{-1}) and 980-1020 cm^{-1} (near 1009 cm^{-1}) were selected. As shown in Table 1, the LSSVM model based on 760–800 cm^{-1} got better performance ($R_P^2 = 0.960$, indicating a high accuracy of the model, and RPD = 5.004 > 3, indicating a very good reliability of the model). Likewise, for carbendazim, spectra of 1200-1235 cm^{-1} (near 1224 cm^{-1}) and 1235–1280 cm^{-1}(near 1260 cm^{-1}) were chosen. The result showed that the LSSVM model based on 1235–1280 cm^{-1} got better results ($R = 0.933$, RPD = 3.504). For chlorpyrifos, spectra of 580–630 cm^{-1} (near 610 cm^{-1}) and 660-690 cm^{-1} (near 675 cm^{-1}) were extracted, which showed that the LSSVM model performed well at 580-630 cm^{-1} ($R_P^2 = 0.864$, RPD = 2.507). It is worth noting that the RPD of chlorpyrifos was less than 3 in both models (Table 1), which might be due to the error caused by sampling rate (Figure 3) and uniformity (Figure S5), as well as the poor affinity between AuNPs and chlorpyrifos molecules. How to further improve the performance of residue detection of various pesticides is the focus of our future work. Thus, the proposed flexible SERS tape has a great potential for high-

efficiency extraction and in situ detection of the target molecules on arbitrary surfaces.

4. Conclusions

In this research, the pesticide residue detection method on tomato surface based on flexible SERS tape was studied from many aspects. With good bendability and viscosity, 3M9080 obtained high and stable sampling efficiency and was selected as an ideal flexible support. By optimizing the experimental parameters, SERS signals were improved in uniformity and sensitivity. Detection limits of thiabendazole, carbendazim, and chlorpyrifos on glass surface were 8, 20, and 40 ng/cm^2, respectively. As a practical application, we undertook semiquantitative detection with a portable Raman spectrometer on tomato surface and realized promising results, indicating that the proposed method could be applied to the rapid nondestructive online semiquantitative detection for different kinds of pesticides, especially in the preliminary screening stage. This study also provides an emerging prospect for the detection of trace contaminations including but not limited to these three pesticides on complex surface.

Data Availability

The data used to support the findings of this study are included within the article and supplementary materials.

Conflicts of Interest

The authors declare that there are no conflicts of interest regarding the publication of this paper.

Acknowledgments

This research was supported by the Science and Technology Department of Guangdong Province (grant no. 2019B020216001) and the Fundamental Research Funds of the Central Universities (grant no. K20210123).

Supplementary Materials

Table S1. The assignment of Raman peaks of thiabendazole. Table S2. The assignment of Raman peaks of carbendazim. Table S3. The assignment of Raman peaks of chlorpyrifos. Table S4. One-way analysis of variance (ANOVA) results of two tapes' sampling rate (3M9080 and scotch tape) in the detection of three pesticides on tomato surface. Figure S1. Commercial tapes: (a) scotch tape; (b) paper tape; (c) 3M Post-it; (d) 3M9080 super tape. Figure S2. Ultraviolet spectrophotometer (UV-VIS) spectra of AuNPs (a) before and (b) after the addition of NaCl. Figure S3. Transmission electron microscopy (TEM) of AuNPs (a) before and (b) after the addition of NaCl; (c)–(e) scanning electron microscopy (SEM) of flexible SERS substrate based on 3M9080 at different magnifications. Figure S4. Linear regression analyses of the selected characteristic peak's intensity and concentration of (a) thiabendazole, (b) carbendazim, and (c) chlorpyrifos. Figure S5. Bar chart for feature peak intensity of each pesticide from 20 random sites on SERS tape. Figure S6. SERS spectra of chlorpyrifos at 1 day and 45 days. (*Supplementary Materials*)

References

[1] J. Costa-Rodrigues, O. Pinho, and P. R. R. Monteiro, "Can lycopene be considered an effective protection against cardiovascular disease?" *Food Chemistry*, vol. 245, pp. 1148–1153, 2018.

[2] H. Sun, H. Liu, and Y. Wu, "A green, reusable SERS film with high sensitivity for in-situ detection of thiram in apple juice," *Applied Surface Science*, vol. 416, pp. 704–709, 2017.

[3] W. Zhong, F. Gao, J. Zou et al., "MXene@Ag-based ratiometric electrochemical sensing strategy for effective detection of carbendazim in vegetable samples," *Food Chemistry*, vol. 360, p. 130006, 2021.

[4] K. H. Wang, M. Z. Huang, J. Chen et al., "A "drop-wipe-test" SERS method for rapid detection of pesticide residues in fruits," *Journal of Raman Spectroscopy*, vol. 49, no. 3, pp. 493–498, 2018.

[5] M. F. Cardinal, E. Vander Ende, R. A. Hackler et al., "Expanding applications of SERS through versatile nanomaterials engineering," *Chemical Society Reviews*, vol. 46, no. 13, pp. 3886–3903, 2017.

[6] S. Laing, K. Gracie, and K. Faulds, "Multiplex in vitro detection using SERS," *Chemical Society Reviews*, vol. 45, no. 7, pp. 1901–1918, 2016.

[7] H. He, D.-W. Sun, H. Pu, L. Chen, and L. Lin, "Applications of Raman spectroscopic techniques for quality and safety evaluation of milk: a review of recent developments," *Critical Reviews in Food Science and Nutrition*, vol. 59, no. 5, pp. 770–793, 2019.

[8] J. Kubackova, G. Fabriciova, P. Miskovsky, D. Jancura, and S. Sanchez-Cortes, "Sensitive surface-enhanced Raman spectroscopy (SERS) detection of organochlorine pesticides by alkyl dithiol-functionalized metal nanoparticles-induced plasmonic hot spots," *Analytical Chemistry*, vol. 87, no. 1, pp. 663–669, 2015.

[9] R. Li, G. Yang, J. Yang, J. Han, J. Liu, and M. Huang, "Determination of melamine in milk using surface plasma effect of aggregated Au@SiO2 nanoparticles by SERS technique," *Food Control*, vol. 68, pp. 14–19, 2016.

[10] W. Zhang, J. Ma, and D.-W. Sun, "Raman spectroscopic techniques for detecting structure and quality of frozen foods: principles and applications," *Critical Reviews in Food Science and Nutrition*, vol. 61, no. 16, pp. 2623–2639, 2021.

[11] B. Fortuni, Y. Fujita, M. Ricci et al., "A novel method for in situ synthesis of SERS-active gold nanostars on polydimethylsiloxane film," *Chemical Communications*, vol. 53, no. 37, pp. 5121–5124, 2017.

[12] H. Kim, B. T. Trinh, K. H. Kim et al., "Au@ZIF-8 SERS paper for food spoilage detection," *Biosensors and Bioelectronics*, vol. 179, p. 113063, 2021.

[13] S. Kumar, P. Goel, and J. P. Singh, "Flexible and robust SERS active substrates for conformal rapid detection of pesticide residues from fruits," *Sensors and Actuators B: Chemical*, vol. 241, pp. 577–583, 2017.

[14] M. Lee, K. Oh, H.-K. Choi et al., "Subnanomolar sensitivity of filter paper-based SERS sensor for pesticide detection by hydrophobicity change of paper surface," *ACS Sensors*, vol. 3, no. 1, pp. 151–159, 2018.

[15] J. Chen, Y. Huang, P. Kannan et al., "Flexible and adhesive surface enhance Raman scattering active tape for rapid

detection of pesticide residues in fruits and vegetables," *Analytical Chemistry*, vol. 88, no. 4, pp. 2149–2155, 2016.

[16] J. L. Jiang, S. M. Zou, L. W. Ma, S. F. Wang, J. S. Liao, and Z. J. Zhang, "Surface-enhanced Raman scattering detection of pesticide residues using transparent adhesive tapes and coated silver nanorods," *ACS Applied Materials & Interfaces*, vol. 10, pp. 9129–9135, 2018.

[17] D. Cialla, S. Pollok, C. Steinbrücker, K. Weber, and J. Popp, "SERS-based detection of biomolecules," *Nanophotonics*, vol. 3, no. 6, pp. 383–411, 2014.

[18] B. Sharma, R. R. Frontiera, A.-I. Henry, E. Ringe, and R. P. Van Duyne, "SERS: materials, applications, and the future," *Materials Today*, vol. 15, no. 1-2, pp. 16–25, 2012.

[19] H. Wu, Y. Luo, C. Hou et al., "Flexible bipyramid-AuNPs based SERS tape sensing strategy for detecting methyl parathion on vegetable and fruit surface," *Sensors and Actuators B: Chemical*, vol. 285, pp. 123–128, 2019.

[20] L. Wang, X. Wang, L. Cheng et al., "SERS-based test strips: principles, designs and applications," *Biosensors and Bioelectronics*, vol. 189, p. 113360, 2021.

[21] Y. Shi, W. Li, X. Feng et al., "Sensing of mercury ions in Porphyra by Copper @ Gold nanoclusters based ratiometric fluorescent aptasensor," *Food Chemistry*, vol. 344, p. 128694, 2021.

[22] A. Hussain, H. B. Pu, and D. W. Sun, "Cysteamine modified core-shell nanoparticles for rapid assessment of oxamyl and thiacloprid pesticides in milk using SERS," *Journal of Food Measurement and Characterization*, vol. 14, no. 4, pp. 2021–2029, 2020.

[23] G. Yao, S. Guo, W. Yu, M. Muhammad, J. Liu, and Q. Huang, "DFT and Raman study of all-trans astaxanthin optical isomers," *Spectrochimica Acta Part A: Molecular and Biomolecular Spectroscopy*, vol. 262, p. 120143, 2021.

[24] L. Huang, Y. Zhou, L. Meng, D. Wu, and Y. He, "Comparison of different CCD detectors and chemometrics for predicting total anthocyanin content and antioxidant activity of mulberry fruit using visible and near infrared hyperspectral imaging technique," *Food Chemistry*, vol. 224, pp. 1–10, 2017.

[25] C. Müller, L. David, V. Chiş, and S. C. Pînzaru, "Detection of thiabendazole applied on citrus fruits and bananas using surface enhanced Raman scattering," *Food Chemistry*, vol. 145, pp. 814–820, 2014.

[26] L. N. Furini, C. J. L. Constantino, S. Sanchez-Cortes, J. C. Otero, and I. López-Tocón, "Adsorption of carbendazim pesticide on plasmonic nanoparticles studied by surface-enhanced Raman scattering," *Journal of Colloid and Interface Science*, vol. 465, pp. 183–189, 2016.

[27] C. Li, C. Yang, S. Xu et al., "Ag2O@Ag core-shell structure on PMMA as low-cost and ultra-sensitive flexible surface-enhanced Raman scattering substrate," *Journal of Alloys and Compounds*, vol. 695, pp. 1677–1684, 2017.

[28] X. Gong, M. Tang, Z. Gong, Z. Qiu, D. Wang, and M. Fan, "Screening pesticide residues on fruit peels using portable Raman spectrometer combined with adhesive tape sampling," *Food Chemistry*, vol. 295, pp. 254–258, 2019.

[29] Y. He, S. P. Xiao, T. Dong, and P. C. Nie, "Gold nanoparticles with different particle sizes for the quantitative determination of chlorpyrifos residues in soil by SERS," *International Journal of Molecular Sciences*, vol. 20, no. 11, p. E2817, 2019.

[30] X.-M. Li, M.-H. Bi, L. Cui et al., "3D aluminum hybrid plasmonic nanostructures with large areas of dense hot spots and long-term stability," *Advanced Functional Materials*, vol. 27, no. 10, Article ID 1605703, 2017.

[31] D. J. Maxwell, S. R. Emory, and S. Nie, "Nanostructured thin-film materials with surface-enhanced optical properties," *Chemistry of Materials*, vol. 13, no. 3, pp. 1082–1088, 2001.

[32] R. Niu, C. Song, F. Gao et al., "DNA origami-based nanoprinting for the assembly of plasmonic nanostructures with single-molecule surface-enhanced Raman scattering," *Angewandte Chemie International Edition*, vol. 60, no. 21, pp. 11695–11701, 2021.

[33] J. Liu, J. N. Chen, Y. J. Dong et al., "The origin of the unusual red-shifted aggregation-state emission of triphenylamine-imidazole molecules: excimers or a photochemical reaction?" *Materials Chemistry Frontiers*, vol. 4, no. 5, pp. 1411–1420, 2020.

[34] Y. Jin, P. Ma, F. Liang, D. Gao, and X. Wang, "Determination of malachite green in environmental water using cloud point extraction coupled with surface-enhanced Raman scattering," *Analytical Methods*, vol. 5, no. 20, pp. 5609–5614, 2013.

[35] E. Wongrat, N. Hongsith, D. Wongratanaphisan, A. Gardchareon, and S. Choopun, "Control of depletion layer width via amount of AuNPs for sensor response enhancement in ZnO nanostructure sensor," *Sensors and Actuators B: Chemical*, vol. 171–172, pp. 230–237, 2012.

[36] Y. Guo, Y. Zhang, H. Shao, Z. Wang, X. Wang, and X. Jiang, "Label-Free Colorimetric detection of cadmium ions in rice samples using gold nanoparticles," *Analytical Chemistry*, vol. 86, no. 17, pp. 8530–8534, 2014.

[37] X. Zhang, M. R. Servos, and J. W. Liu, "Instantaneous and quantitative functionalization of gold nanoparticles with thiolated DNA using a pH-assisted and surfactant-free route," *Journal of the American Chemical Society*, vol. 134, no. 17, pp. 7266–7269, 2012.

[38] G. Kwon, J. Kim, D. Kim, Y. Ko, Y. Yamauchi, and J. You, "Nanoporous cellulose paper-based SERS platform for multiplex detection of hazardous pesticides," *Cellulose*, vol. 26, no. 8, pp. 4935–4944, 2019.